A CNN-RNN based approach for Simultaneous Detection, Identification and Classification of Intracranial Hemorrhage

Prishita Kadam
B.E Student, Computer Engineering
St. Francis Institute of Technology
Mumbai, India
prishitakadam12@gmail.com

Jesdin Raphael
B.E Student, Computer Engineering
St. Francis Institute of Technology
Mumbai, India
jesdinraphael@gmail.com

Prajwal Karale
B.E Student, Computer Engineering
St. Francis Institute of Technology
Mumbai, India
prajwalkarale0508@gmail.com

Ian Dsilva
B.E Student, Computer Engineering
St. Francis Institute of Technology
Mumbai, India
dsilvaian2000@gmail.com

Kavita Sonawane
Professor, Computer Engineering
St. Francis Institute of Technology
Mumbai, India
kavitasonawane@sfit.ac.in

Abstract*—Intracranial Hemorrhage (ICH) refers to bleeding inside the brain or skull and is considered a life-threatening condition as the accumulation of blood can lead to increased intracranial pressure, which can crush delicate brain tissues or limit its blood supply. ICH accounts for 10 to 20% of all strokes and requires immediate diagnosis and treatment. In this study, our main aim was to precisely detect and classify Intracranial Hemorrhage simultaneously. The use of Recurrent Neural Network (RNN) in analysing the sequential information obtained from slice-level classifications has been proved to be beneficial [1]. Our proposed architectures combined a Convolution Neural Network (CNN) and a Recurrent Neural Network (RNN) i.e. CNN with Long Short Term Memory (LSTM) and CNN with Gated Recurrent Unit (GRU). Using RNN would enable the previously ignored small features to be easily detected while simultaneously improving the model's capability to distinguish between the subtypes of Intracranial Hemorrhage. Also, by performing windowing in preprocessing certain features not previously visible would become clearer. This led to the framework of three architectures: Xception, Xception-LSTM, and Xception-GRU. The dataset collected by the Radiological Society of North America is used to train these architectures (RSNA) [2]. The dataset consisted of 752,803 DICOM files out of which 10% of randomly selected samples were used for testing. The performance of these architectures is evaluated and compared using different parameters like Loss, Accuracy, AUC-ROC score, Precision, Sensitivity, Specificity, and F1 Score. We found out Xception GRU outperformed the other two architectures in almost all the parameters having achieved the loss of 0.0659. Furthermore, we have also performed a detailed analysis of per-class results using the same parameters. We believe that the use of CNN-RNN architecture increases the accuracy of ICH detection, identification and classification which would help reduce diagnosis errors

***Index Terms*—Intracranial Hemorrhage, Image Processing, Convolutional Neural networks, Recurrent Neural Networks, Classification, Deep Learning, CNN-RNN**

I. Introduction

Intracranial Hemorrhage (ICH) occurs in a variety of patients suffering from high blood pressure, stroke, vascular abnormalities, aneurysm, blood clotting disorders, and trauma [2], [3]. Depending on their shape, location, and size, different types of ICH can be identified. It is essential to diagnose ICH, preferably within 24 hours to reduce patient mortality [3]. The overall incidence of spontaneous Intracerebral Hemorrhage, a type of Intracranial Hemorrhage, occurs roughly about 40,000 to 67,000 cases per year in the United States and around 24.6 per 100,000 worldwide [4]–[7]. The death rate over 30 days is between 35% to 52%, and only 20% of survivors are expected to have a complete functional recovery at 6 months [6]. Hence, creating the requirement of high accuracy for the detection and classification for the treatment of ICH.

To determine the identity, location, and subtype of the ICH, trained radiologists review anatomical photographs of the patient's cranium. [9]. This process, however, is complicated and often time consuming [8]. Computerized detection of ICH using patient's CT Scan could identify it earlier and more accurately, which would thus improve clinical outcomes. Furthermore, a computerized diagnostic tool like this would help enhance radiologists' performance by providing them with a "second opinion" in a cost-effective manner [9].

The performance bar for correctly interpreting head CT scans is very high and is considered as a core skill in radiological training problems, with most of the skilled readers, demonstrating sensitivity/specificity between 0.95 and 1.00 [10]. The applicability of machine learning models like neural networks for medical image processing has been increased due to advances in image recognition [3]. Meaningful patterns and features within large datasets can be recognized using

Deep Learning Systems without any explicit directions [3]. To create an accurate deep learning algorithm for radiology, we need a large number of precisely labeled CT scans as well as appropriate model architectures [11].

In this study, we have shown how Recurrent Neural Networks can be stacked with Convolutional Neural Network to efficiently detect and classify Acute Intracranial Hemorrhage using deep learning algorithms. This would help to shorten the diagnosis time as well as to reduce diagnosis errors. Our focus is on the classification of five types of Intracranial Hemorrhage: Intraparenchymal Hemorrhage (IPH), Intraventricular Hemorrhage (IVH), Subarachnoid Hemorrhage (SAH), Subdural Hemorrhage (SDH), and Epidural Hemorrhage (EDH).

The rest of the paper is organized as followed: Section II covers existing research in the area. Section III highlights the challenges identified. Section IV describes the data and preprocessing technique used, the different types of models that have been proposed in this study as well as the different parameters used to evaluate the models. The observations and results are discussed in section V. In Section VI we conclude and discuss the future work of our study.

II. Related Works

Deep Learning models are widely used in computer vision and can achieve high accuracy on image recognition and classification, sometimes exceeding human-level performance [12]. Over the years, different algorithms in deep learning have been proposed to identify and classify various types of Intracranial Hemorrhage. For more complex identification, machine learning results were also validated by human specialists [13], [14] Chilamkurthy et. al. assembled a dataset containing 313,318 head CT scans along with their medical reports from around 20 centers in India to develop and validate algorithms using deep learning for automated identification of ICH and its types. The performance of their algorithm, when compared with three radiologists, came out to be higher [3]. Their study suggested that deep learning algorithms could be a helpful supplement for the identification of Head CT finding in a trauma setting, providing a lower bound for performance in terms of quality and consistency of radiological inference [14]. [3] T. Lewick et. al. proposed a deep learning approach that consisted of CNN architecture onto which a 2 layer fully-connected classifier was stacked. Their model was able to analyze single frame CT scans with comparative accuracy to a radiologist.

[15] S. P. Singh et. al. proposed a method for normalizing 3D volumetric scans using the intensity profile of the training samples which aids the CNN by creating a higher contrast around the abnormal region of interest. The proposed shallow 3D CNN required fewer training epochs, fewer trainable parameters, and higher accuracy compared to 3D VGGNet and 3D ResNet. Previous methods usually assumed that all classifiers shared the same image features to predict multiple labels, in order to avoid problems like overfitting [16], due to which objects that are small in the images were easily ignored or became hard to recognize independently [17]. These small objects although being hard to recognize by themselves can easily be inferred given enough contexts. Keeping this in mind, many studies have proposed CNN-LSTM models.

A study incorporating Convolutional Neural Network and Recurrent Neural Network by means of Bidirectional LSTM was proposed by A. Patel et. al. [1]. They demonstrated the viability of end-to-end training of a CNN based upon image-level annotations of high-resolution non-contrast CT scans, for accurate image-level classification [1]. Their study proved to be better than several approaches that were implemented using only the 2D output of the CNN. Similarly, [9] Ko. H. et. al. developed a predictive deep learning model using both CNN and LSTM networks based on a single head computed tomography (CT) image. They used image augmentation techniques to balance their dataset and achieved the weighted multi-label log loss of 0.07528. [18] D. Guo et. al. proposed a method that contained a shared encoder to extract features for both classification and segmentation tasks while utilizing a convolutional long short-term memory (ConvLSTM) [19] module to capture the sequential information embedded in consecutive slices. Unlike region proposal based approaches, such as mask R-CNN, that relies on instance level subtype labels, their network was able to be trained with slice level labels, offering more flexibility.

III. Challenges identified

A. Class Accuracy:

Previous studies achieved good performance for detection of ICH but poor performance in regards to the ability to distinguish between the types of hemorrhage.

B. Same Image Features used for Multi-Label Classification:

Same image features being used to identify all images for multiclass classification leading to small unique objects being disregarded [17].

C. Windowing:

Due to windowing being neglected there is a loss in the number of features visible.

IV. Methodology

A. Data Pre-processing

To view CT scans, windowing is used to transform HU values into grayscale ([0, 255]) values. This enhances the visibility of the different features of tissues while also emphasizing the tissues of interest by maximizing subtle differences among the tissues.Windowing is defined by two parameters: window level (WL) and window width (WW) [20].

We have used three different windows for this process along with the following settings: (a) Brain window (WL=40, WW=80) to distinguish among different types of soft tissues [20] (b) Blood/Subdural window (WL=80, WW=200) which is useful for delineating blood and subdural fluid [20] (c) Bone Window (WL=600, WW=2800) helps to visualize details of bone structures and identify fine skull lesions [20]. With the help of these settings, only the tissues with desired Hounsfield

units (HU) are mapped into the three channels of the input tensor [3]. The same is shown in Fig. 1.

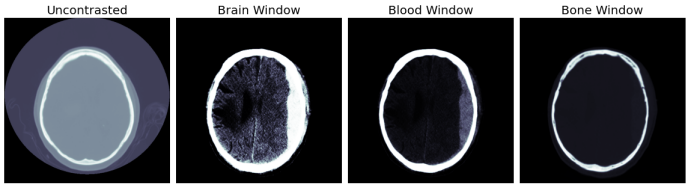

Fig. 1. Windowing (From Left to Right): Uncontrasted Scan, Brain Window, Blood/Subdural Window, Bone Window

B. Model Description

CNN has been found to be a powerful tool in analyzing spatial image storage information but they lack performance in learning dependencies across sequential information. RNNs are capable of retaining the information that is present in the form of sequences. Therefore, we propose the models that are the combination of a convolutional neural network and different recurrent neural networks.

1) *Xception Architecture:*
We have used the Xception model which is a deep CNN architecture as our backbone model forming a base for feature extraction from the given input data. The architecture consists of 36 convolution layers which are divided into 14 modules [9]. Except for first and last modules, all have residual connections between them. [9]. The architectural diagram of the Xception model is shown in [9] Fig. 2. The main reason for using the Xception model as the backbone architecture is that it solely relies on depthwise separable convolutions which is a good alternative to classical convolutions, since the number of multiplications needed is far lower in depth-wise separable convolutions than in classical convolutions, resulting in a faster calculation period [21].
2) *Xception LSTM and Xception GRU Architecture:*
A recurrent neural network is a special kind of artificial neural network that consists of loops making it possible to store information within the network. In nutshell, recurrent neural networks use their reasoning from past experiences to inform future events. Standard RNN architecture cannot be directly used in sequences where the input is spatial. So in order to accomplish the tasks which require image sequences to predict a result, we require a more sophisticated architecture. Hence we opt for the CNN-RNN architecture.
   a) *LSTM:*
   Long Short Term Memory (LSTM) is a RNN that uses a particular kind of cell that helps to memorize long-term dependencies by having gateways that pass through different cells. A LSTM cell is formed by adding three gates to a RNN neuron. The three gates added are: Forget Gate, Input Gate, and Output Gate. These gates help the LSTM cell to learn the long time dependency of a sequence and also helps to deal with vanishing gradient problems that occur in standard RNN. The LSTM cell can be represented by using the following equations [22] Eq. (1):

$$\begin{aligned} i_t &= \sigma(W_i x_t + U_i h_{t-1} + b_i) \\ f_t &= \sigma(W_f x_t + U_f h_{t-1} + b_f) \\ o_t &= \sigma(W_o x_t + U_o h_{t-1} + b_o) \\ \check{C} &= tanh(W_c x_t + U_c h_{t-1} + b_c) \\ C_t &= f_t \odot C_{t-1} + i_t \odot \check{C}_t \\ h_t &= o_t \odot tanh(C_t) \end{aligned} \tag{1}$$

   b) *GRU:*
   The GRU cell is similar to the LSTM cell, but with a few important differences. The number of gates present in the GRU cell are less than that of LSTM. GRU uses the hidden state for transferring information. Since the number of gates in the GRU cell is less, the number of parameters are reduced due to which it has few tensor operations which makes it faster than LSTM and thus increases the performance of the model. In GRU, the gating signals are reduced to two from the LSTM model [23]. The two gates are: Update Gate z_t and Reset Gate r_t. GRU Model can be represented as follows in [23] Eq. (2, 3):

$$h_t = (1 - z_t) \odot h_{t-1} + z_t \odot \tilde{h_t} \tag{2}$$

$$\tilde{h_t} = g(W_h x_t + U_h(r_t \odot h_{t-1}) + b_h) \tag{3}$$

   And the two gates are shown in [23] Eq. (4, 5):

$$z_t = \sigma(W_z x_t + U_z h_{t-1} + b_z) \tag{4}$$

$$r_t = \sigma(W_r x_t + U_r h_{t-1} + b_r) \tag{5}$$

   c) *CNN-RNN Implementation:*
   The architecture of the model that we propose is shown in Fig. 3. We have used the Xception model as a backbone of our proposed architecture whose diagram is shown in Fig 3. Keeping the base architecture the same, we have implemented two different CNN-RNN architectures, Xception LSTM and Xception GRU as shown in Fig. 3A and Fig. 3B respectively. In the CNN-RNN architecture, the first part of the network which is a CNN network takes an input image of 256x256x3, which is then fed into the Xception architecture that consists of an entry flow, a middle flow which is iterated over eight times, and finally an exit flow. The second half of the proposed architecture consists of two stacked RNN Layers (LSTM or GRU) which have 512 units and the output of these layers is then multiplied with the output of the

CNN network. The final output is then the fully connected layer having 6 nodes with the sigmoid activation function and a dropout rate of 0.20.

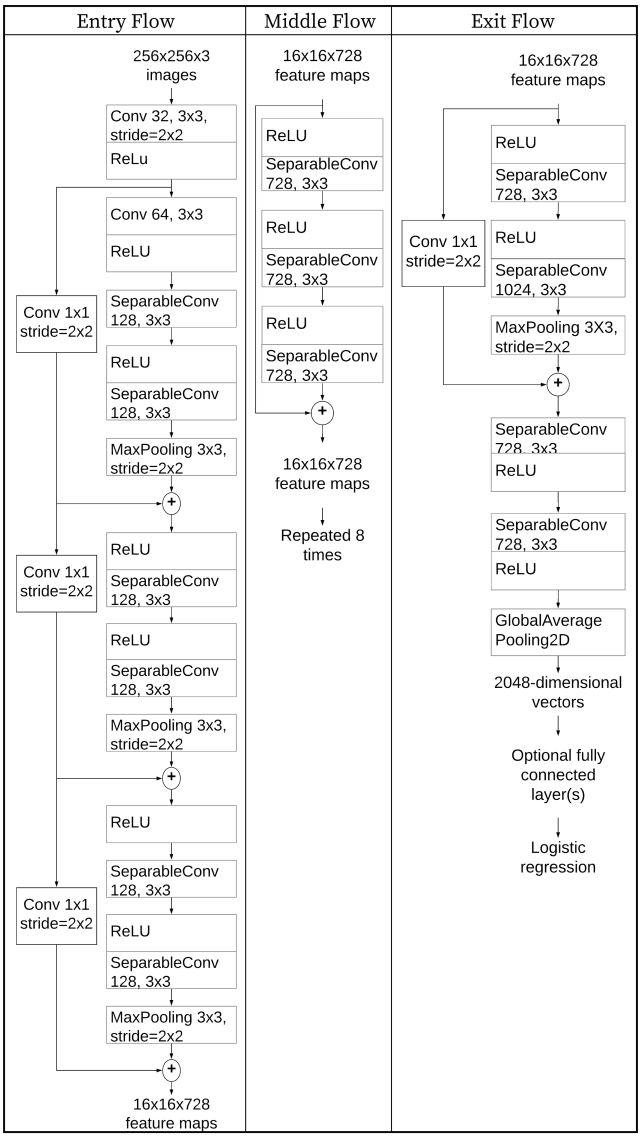

Fig. 2. Xception Base Model

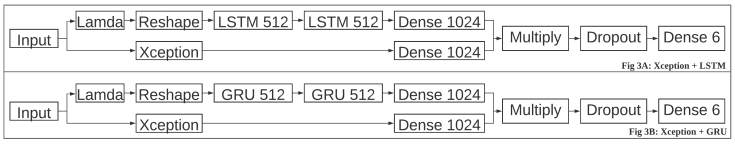

Fig. 3. Xception LSTM and Xception GRU Model

C. Experimental Set-Up

All Proposed models are experimented with common data sets so that we can compare and evaluate the performances and uniformly analyze the behavior of each model.

1) *Dataset:* The dataset for our study was obtained by the Radiological Society of North America (RSNA) [2]. Fig. 4 shows sample images of different types of hemorrhage present in our dataset which consists of a total of 752,803 labeled DICOM files. Within the dataset, approximately 10% of samples are diagnosed with hemorrhage and approximately 85% of images contain no hemorrhage at all. Additionally, a list of image IDs and multiple labels, one for each of five subtypes, as well as an additional label 'any', which will be true if one or more of the sub-type labels are true, is provided in a csv file. There are six rows per image ID, each with a label that indicates the likelihood of all types of hemorrhage being present in the image [2].
For testing, we kept aside 10% of randomly selected examples from the same dataset.

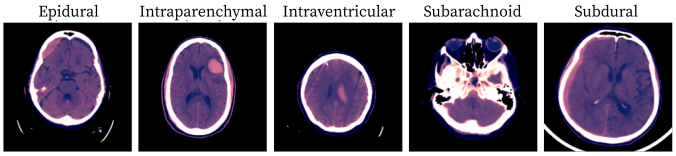

Fig. 4. Sample Images of Different types of Hemorrhages

2) *Evaluation Metrics:*

a) *Accuracy:* It is a proportion of the system's correct predictions for the overall number of predictions. It determines how often the classifier would show the correct output. Represented in equation (6).

$$Accuracy = \frac{TP + TN}{TP + TN + FP + FN} \quad (6)$$

b) *AUC (Area Under the Curve)*: It is a visualization graph used to analyze the efficiency of various machine learning models. This graph is a graph of sensitivity to specificity. The region under the curve (AUC) shows us how effective a model is when we talk about its potential to generalize.

c) *Precision:* It is the proportion of True Positives divided by the number of True Positive and False Positive. Represented in equation (7).

$$Precision = \frac{TP}{TP + FP} \quad (7)$$

d) *Sensitivity:* It is the ratio of patients with the disease that have been tested positive. It informs us of the proportion of actual positive cases which have been projected as positive by our model. Represented in equation (8).

$$Sensitivity = \frac{TP}{TP + FN} \quad (8)$$

e) *Specificity:* It is the ratio of patients with the disease that have been tested negative. It informs us of the proportion of actual negative cases which have been projected as negative by our model. Represented in equation (9).

$$Specificity = \frac{TN}{TN + FP} \tag{9}$$

f) *F1 Score:* It is used to test binary classification systems that classify examples as 'positive' or 'negative'. It is the harmonic mean of precision and recall of the model. Represented in equation (10).

$$F1 = 2 * \frac{Precision * Recall}{Precision + Recall} \tag{10}$$

V. RESULTS AND DISCUSSION

For comparing the performance of Xception, Xception GRU, and Xception LSTM we have evaluated the models based on the Accuracy, ROC AUC, Precision, Sensitivity, Specificity, and F1 Score as mentioned in Table I and II.

TABLE I
RESULTS OBTAINED FOR XCEPTION, XCEPTION LSTM, AND XCEPTION GRU MODELS

Parameters	Xception	Xception LSTM	Xception GRU
Loss	0.0753	0.0708	0.0659
Accuracy	0.9737	0.9748	0.9764
AUC	0.9744	0.9761	0.9785
Precision	0.8503	0.8646	0.8427
Sensitivity	0.6667	0.6738	0.7317
Specificity	0.9927	0.9935	0.9915
F1 Score	0.7474	0.7574	0.7833

Observation: Xception GRU results in the best performance

Based on Table 1 we can deduce that the results of Xception GRU model has better performance on most of the metrics as compared to the Xception and Xception LSTM models with accuracy as high as 97.64%. Fig 5 shows the AUC score of the detection of the subtypes. The high AUC score shows that it is more capable of distinguishing between the different classes.

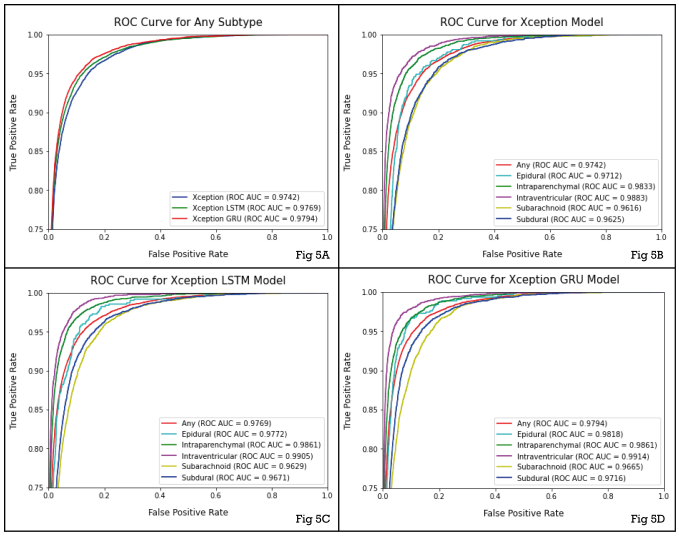

Fig. 5. ROC AUC curves for Xception, Xception LSTM and Xception GRU Models.

Fig 5A clearly illustrates that the overall capability of the Xception GRU model is better than the other two models. Fig 5b, 5c, 5d depicts the ROC AUC curve of the individual models shows evidently that even for a specific subclass the effectiveness of distinguishing the subclass is the best in the Xception GRU Model.

From Tables I and II, we can notice that the Xception model has the lowest results for all parameters. Where the Xception LSTM model shows better results compared to Xception but shows poorer results compared to Xception GRU, which shows

TABLE II
CLASS WISE RESULTS OF XCEPTION, XCEPTION LSTM, AND XCEPTION GRU MODELS

Architecture	Parameters	Per Class Results					
		Any	Epidural	Intraparenchymal	Intraventricular	Subarachnoid	Subdural
Xception	Accuracy	0.9522	0.9928	0.9797	0.9873	0.9693	0.9613
	ROC AUC	0.9742	0.9712	0.9833	0.9883	0.9616	0.9625
	Precision	0.9829	0.9989	0.9908	0.9945	0.9944	0.9936
	Sensitivity	0.9619	0.9939	0.9879	0.9924	0.9740	0.9660
	Specificity	0.8859	0.6721	0.8092	0.8377	0.8087	0.8369
	F1 Score	0.9723	0.9964	0.9894	0.9934	0.9841	0.9796
Xception LSTM	Accuracy	0.9543	0.9936	0.9814	0.9865	0.9695	0.9638
	ROC AUC	0.9769	0.9772	0.9861	0.9905	0.9629	0.9671
	Precision	0.9874	0.9995	0.9923	0.9983	0.9879	0.9945
	Sensitivity	0.9603	0.9941	0.9882	0.9879	0.9802	0.9677
	Specificity	0.9119	0.8296	0.8361	0.9334	0.7152	0.8630
	F1 Score	0.9736	0.9968	0.9903	0.9931	0.9840	0.9809
Xception GRU	Accuracy	0.9567	0.9935	0.9823	0.9886	0.9718	0.9655
	ROC AUC	0.9794	0.9818	0.9861	0.9914	0.9665	0.9716
	Precision	0.9809	0.9984	0.9944	0.9949	0.9922	0.9870
	Sensitivity	0.9688	0.9951	0.9871	0.9932	0.9785	0.9764
	Specificity	0.8798	0.6789	0.8716	0.8535	0.7857	0.7711
	F1 Score	0.9748	0.9967	0.9907	0.9941	0.9853	0.9817

Observation: For almost all Parameters Xception GRU results in the best per class results.

high detection efficiency and ICH classification.

Table II shows the performance of all the architectures for the multi-class environment. Xception GRU shows an overall better performance for all the classes.

Additionally, The GRU has a smaller number of tensor operations hence, it requires fewer computations, which makes it faster than the LSTM.

VI. Conclusion and Future Scope

During our research, our primary focus was on increasing the overall performance of the Xception Model using RNN. Our Dataset was obtained from Kaggle which was made available by the Radiological Society of North America (RSNA) [2] consisting of 752,803 images as mentioned in Section III C. For testing, we used 10 % of the total dataset. To increase the visibility of the CT scans windowing was performed. Here, we have used three windows to perform this which are the Brain Window, the Blood Window, and the Bone Window as mentioned in Section III A. Based on the results obtained by testing the Models we can conclude the following:

1) **Capability:** Xception GRU model outperforms both Xception as well as Xception LSTM models
2) **Speed:** Though Training on RNN is slower than that on CNN models the better performance outweighs it. Also, speed wise GRU trains faster than LSTM due to the lower number of parameters
3) **Comprehensibility:** The proposed model is efficient and easy to implement

In light of the above points, it can be concluded that Xception with stacked GRU layers can increase the performance of the classification.

By optimizing the preprocessing techniques and by using Bi-directional Layers for GRU and LSTM network, the performance of the model can be further enhanced.

References

[1] A. Patel, S. C. van de Leemput, M. Prokop, B. Van Ginneken and R. Manniesing, "Image Level Training and Prediction: Intracranial Hemorrhage Identification in 3D Non-Contrast CT," in IEEE Access, vol. 7, pp. 92355-92364, 2019, doi: 10.1109/ACCESS.2019.2927792.

[2] Kaggle and RSNA, "Intracranial hemorrhage detection dataset," 2019. [Online]. Available: https://www.kaggle.com/c/rsna-intracranial-hemorrhage-detection/data.

[3] T. Lewick, M. Kumar, R. Hong and W. Wu, "Intracranial Hemorrhage Detection in CT Scans using Deep Learning," 2020 IEEE Sixth International Conference on Big Data Computing Service and Applications (BigDataService), Oxford, UK, 2020, pp. 169-172, doi: 10.1109/BigDataService49289.2020.00033.

[4] C. J. van Asch, M. J. Luitse, G. J. Rinkel, I. van der Tweel, A. Algra, and C. J. Klijn, "Incidence, case fatality, and functional outcome of intracerebral haemorrhage over time, according to age, sex, and ethnic origin: a systematic review and meta-analysis," The Lancet Neurology, vol. 9, no.2, pp. 167-176, 2010.

[5] M. I. Aguilar, and W. D. Freeman, "Spontaneous intracerebral hemorrhage." pp. 555-564.

[6] J. Broderick, S. Connolly, E. Feldmann, D. Hanley, C. Kase, D. Krieger, M. Mayberg, L. Morgenstern, C. S. Ogilvy, and P. Vespa, "Guidelines for the Management of Spontaneous Intracerebral Hemorrhage in Adults: 2007 Update: A Guideline From the American Heart Association/American Stroke Association Stroke Council, High Blood Pressure Research Council, and the Quality of Care and Outcomes in Research Interdisciplinary Working Group: The American Academy of Neurology affirms the value of this guideline as an educational tool for neurologists," Stroke, vol. 38, no. 6, pp. 2001-2023, 2007.

[7] J. A. Caceres, and J. N. Goldstein, "Intracranial hemorrhage," Emergency medicine clinics of North America, vol. 30, no. 3, pp. 771, 2012.

[8] T. Vedin, S. Svensson, M. Edelhamre, M. Karlsson, M. Bergenheim, and P.-A. Larsson, "Management of mild traumatic brain injury–trauma energy level and medical history as possible predictors for intracranial hemorrhage," European Journal of Trauma and Emergency Surgery, vol. 45, no. 5, pp. 901-907, 2019.

[9] H. Ko, H. Chung, H. Lee and J. Lee, "Feasible Study on Intracranial Hemorrhage Detection and Classification using a CNN-LSTM Network," 2020 42nd Annual International Conference of the IEEE Engineering in Medicine & Biology Society (EMBC), 2020, pp. 1290-1293, doi: 10.1109/EMBC44109.2020.9176162.

[10] Kuo W, Häne C, Mukherjee P, Malik J, Yuh EL. Expert-level detection of acute intracranial hemorrhage on head computed tomography using deep learning. Proc Natl Acad Sci U S A 2019;116(45):22737–22745.

[11] Litjens G, Kooi T, Bejnordi BE, Setio AAA, Ciompi F, Ghafoorian M, van der Laak JAWM, van Ginneken B, Sánchez CI. A survey on deep learning in medical image analysis. Med Image Anal. 2017 Dec;42:60-88. doi: 10.1016/j.media.2017.07.005. Epub 2017 Jul 26. PMID: 28778026.

[12] Sushma L, Dr. K. P. Lakshmi, 2020, An Analysis of Convolution Neural Network for Image Classification using Different Models, INTERNATIONAL JOURNAL OF ENGINEERING RESEARCH & TECHNOLOGY (IJERT) Volume 09, Issue 10 (October 2020).

[13] P. Rajpurkar, A. Y. Hannun, M. Haghpanahi, C. Bourn, and A. Y. Ng, "Cardiologist-level arrhythmia detection with convolutional neural networks," CoRR, vol. abs/1707.01836, 2017. [Online]. Available: http://arxiv.org/abs/1707.01836.

[14] S. Chilamkurthy et al., "Deep learning algorithms for detection of critical findings in head CT scans: a retrospective study," The Lancet, vol. 392, no. 10162, pp. 2388–2396, Dec. 2018, doi: 10.1016/S0140-6736(18)31645-3.

[15] S. P. Singh, L. Wang, S. Gupta, B. Gulyás and P. Padmanabhan, "Shallow 3D CNN for Detecting Acute Brain Hemorrhage from Medical Imaging Sensors," in IEEE Sensors Journal, doi: 10.1109/JSEN.2020.3023471.

[16] Y. Wei, W. Xia, J. Huang, B. Ni, J. Dong, Y. Zhao, and S. Yan. Cnn: Single-label to multi-label. arXiv preprint arXiv:1406.5726, 2014.

[17] Wang, J., Yang, Y., Mao, J., Huang, Z., Huang, C., & Xu, W. (2016). CNN-RNN: A unified framework for multi-label image classification. arXiv 1604.04573.

[18] D. Guo et al., "Simultaneous Classification and Segmentation of Intracranial Hemorrhage Using a Fully Convolutional Neural Network," 2020 IEEE 17th International Symposium on Biomedical Imaging (ISBI), Iowa City, IA, USA, 2020, pp. 118-121, doi: 10.1109/ISBI45749.2020.9098596.

[19] Jianxu Chen et al., "Combining fully convolutional and recurrent neural networks for 3d biomedical image segmentation," arXiv:1609.01006, 2016.

[20] Z. Xue, S. Antani, L. R. Long, D. Demner-Fushman, and G. R. Thoma, "Window Classification of Brain CT Images in Biomedical Articles," AMIA Annual Symposium Proceedings, vol. 2012, pp. 1023–1029, Nov. 2012, [Online]. Available: https://www.ncbi.nlm.nih.gov/pmc/articles/PMC3540547/.

[21] F. Chollet, "Xception: Deep Learning with Depthwise Separable Convolutions," 2017 IEEE Conference on Computer Vision and Pattern Recognition (CVPR), Honolulu, HI, USA, 2017, pp. 1800-1807, doi: 10.1109/CVPR.2017.195.

[22] G. E. Dahl, T. N. Sainath and G. E. Hinton, "Improving deep neural networks for LVCSR using rectified linear units and dropout," 2013 IEEE International Conference on Acoustics, Speech and Signal Processing, Vancouver, BC, Canada, 2013, pp. 8609-8613, doi: 10.1109/ICASSP.2013.6639346.

[23] R. Dey and F. M. Salem, "Gate-variants of Gated Recurrent Unit (GRU) neural networks," 2017 IEEE 60th International Midwest Symposium on Circuits and Systems (MWSCAS), Boston, MA, USA, 2017, pp. 1597-1600, doi: 10.1109/MWSCAS.2017.8053243.